

## CONTRIBUTION OF DIFFERENT HARDENING MECHANISMS DURING COLD WORKING OF AISI 304L AUSTENITIC STAINLESS STEEL

The contributions of work-hardening of austenite and the presence of martensite on the hardening of an AISI 304L stainless steel were evaluated based on plastic deformation under different reductions in thickness at two rolling temperatures. The cold deformation temperatures of 300 K and 373 K were chosen to induce strain-hardening plus strain-induced martensitic transformation in the former and strain-hardening in the latter. This made it possible to elucidate the real effects of strengthening mechanisms of metastable austenitic stainless steels during mechanical working.

*Keywords:* stainless steels; deformation-induced martensite; work hardening

### 1. Introduction

Austenitic stainless steels have attracted a considerable attention due to their versatile features such as excellent corrosion resistance, good toughness and acceptable weldability. On the other hand, the strength of these steels is relatively low in the annealed state, which is a drawback for many potential applications. Owing to this deficiency, various methods such as grain refinement by recrystallization [1-3] or reversion of martensite [4-13], solid solution strengthening by adding nitrogen or other elements [14], and cold working through work hardening of austenite and strain-induced martensitic transformation [15] have been practiced so far.

Depending on the steel composition, the temperature of cold working, amount of deformation, and other factors, some strain-induced martensite can be formed, which causes a dramatic increase in the yield strength [16,17]. With increasing deformation temperature, the amount of martensite decreases, and above a specific temperature, martensite is no longer able to form [17]. Moreover, work hardening of the retained austenite can contribute to the strengthening of the steel. As indicated before, despite corrosion resistance and weldability, many industries need materials with high strength. Cold working might be used for this purpose at temperatures that martensite do not form. The work hardening of retained austenite and strain-induced martensitic transformation provide the required strength. Other mechanisms, such as transformation-induced plasticity (TRIP) effect of the austenite [18,19], can insure the good formability of the material.

The work hardening of the retained austenite has been usually neglected in the reported literature. However, in many cases,

there is a considerable amount of retained austenite after cold working [6,9], and hence, the contributions of work hardening and martensitic transformation on the hardening behavior of austenitic stainless steels need to be studied. The present paper aims to deal with this subject based on hardness measurements.

### 2. Experimental details

An AISI 304L stainless steel with the chemical composition (wt%) of 0.02C-18.46Cr-8.07Ni-1.49Mn was used in this study. The average grain size of the as-received material was found to be ~14  $\mu\text{m}$ . After immersing the sheets in a mixture of water and ice (273 K), multi-pass cold rolling with different reductions in thickness of 20, 40, and 60% was performed to achieve various amounts of strain-induced martensite. Moreover, cold rolling using the same reductions in thickness was also conducted on the as-received material after pre-heating of the sheets at relatively low temperature of 373 K [17] to suppress the formation of strain-induced martensite, which makes it possible to study the work-hardening effects, solely. This temperature is low enough to insure that the work-hardening characteristics of austenite will not change considerably ( $T/T_M = 0.21$ , where  $T_M$  is the melting point expressed in Kelvin).

To reveal the grain boundaries, electro-etching was carried out in a 60%  $\text{HNO}_3$  solution at 2 V [20] preceded by electrolytic polishing in a mixture of  $\text{H}_3\text{PO}_4$  and  $\text{H}_2\text{SO}_4$  at 40 V [6]. Subsequently, an Olympus Vanox optical microscope was used for microstructural analysis. The Vickers hardness measurements were applied using a force of 1 kg. The error bars were not shown

\* UNIVERSITY OF TEHRAN, COLLEGE OF ENGINEERING, SCHOOL OF METALLURGY AND MATERIALS ENGINEERING, P.O. BOX 11155-4563, TEHRAN, IRAN

<sup>#</sup> Corresponding author: hmirzadeh@ut.ac.ir

on the figures for the sake of clarity but it is declared that the standard deviation of hardness measurements was lower than 7 HV. X-ray diffraction using a Philips PW-3710 diffractometer with Cu-K $\alpha$  radiation was used for phase analysis. Considering the intensities of  $\gamma(220)$  and  $\gamma(311)$  for austenite in the form of  $0.65(I_{(311)\gamma} + I_{(220)\gamma})$ , and that of  $\alpha'(211)$  for martensite, the volume fraction of martensite can be calculated using the following semi-empirical relationship [6,21]:

$$f_{\alpha'} = \frac{I_{(211)\alpha'}}{I_{(211)\alpha'} + 0.65(I_{(311)\gamma} + I_{(220)\gamma})} \quad (1)$$

### 3. Results

As it is shown in the micrographs of Figure 1a, the grains become elongated as the reduction in thickness increases. The difference in stretching is due to the diversity in amount of rolling strain. It can be seen that due to the low homologous temperature of rolling at 373 K ( $T/T_M = 0.21$ ), the elongation of grains at 373 K is comparable to that observed at 300 K ( $T/T_M = 0.17$ ). In fact, it is presumed in the present work that the work-hardening of austenite induced during rolling at 373 K is comparable to

rolling at 300 K. The used etching method is capable to reveal the grain boundaries but the presence of martensite should be studied based on phase analyzing techniques.

The XRD patterns of the as-received and deformed sheets are depicted in Figure 1b. While the as-received sheet shows only the presence of austenite phase, the pattern of the 20% cold rolled sheet at 300 K shows both austenite and martensite peaks. By increasing the reduction in thickness, a decline in the amount of austenite can be discerned based on the decrease in the austenite peak intensities. This can be also verified based on Eq. (1), where the amount of martensite increases by increasing the reduction in thickness. The XRD peaks of the 60% cold rolled sheet at 373 K are also shown in Figure 1b, which reveals that the intensity of martensite peaks are very low. Therefore, it can be deduced that the strain-induced martensitic transformation does not contribute to hardening of the sheets rolled at 373 K. The quantitative analysis of martensite fraction based on Eq. (1) as shown in Figure 1c is in agreement with the abovementioned findings.

Figure 1c also shows the measured values of hardness for different sheets versus rolling reduction. It can be seen that by increasing the reduction in thickness, hardness increases signifi-

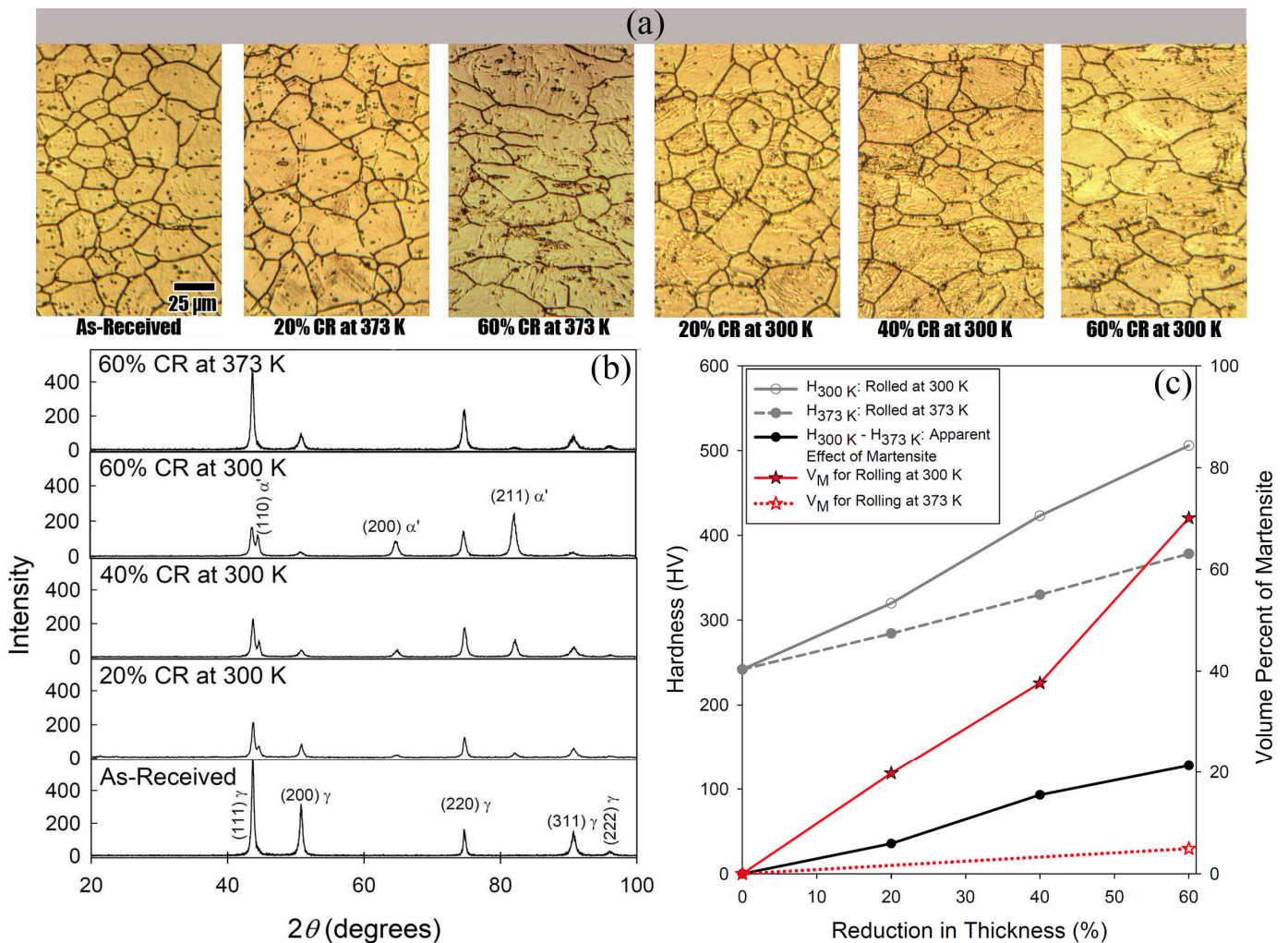


Fig. 1. Obtained results: (a) optical micrographs, (b) XRD patterns, and (c) the results of quantitative phase analysis and hardness measurements of the as-received and rolled sheets

cantly, which can be attributed to strain hardening at 300 K and 373 K and the increase in the amount of martensite at 300 K. It is obvious that the increase in hardness is much more pronounced for samples rolled at 300 K, which can be related to the increase in the amount of martensite by increasing the rolling reduction. Therefore, the difference of hardness values at 300 K and 373 K increases by increasing reduction in thickness, which is shown by a black solid line in Figure 1c. This difference can be considered as the effect of martensite on increasing hardness. However, this is an apparent effect because the work hardening of austenite also takes part in increasing hardness of samples rolled at 300 K. Figure 1c shows that the hardening of the sheets at 373 K is significant, which reveals that the work-hardening of austenite should be taken into consideration. This will be discussed in the following section.

#### 4. Discussion

The work-hardening effect of austenite in the samples rolled at 300 K can be evaluated based on the hardness of samples rolled at 373 K. However, it should be realized that the amount of austenite in the samples rolled at 300 K decreases by increasing rolling reduction, which should be taken into account. For this purpose, the following relation was considered:

$$\Delta H_{\gamma} = (H_{373} - H_0)(1 - V_M) \quad (2)$$

where  $\Delta H_{\gamma}$  is the hardening due to work hardening of austenite,  $H_{373}$  is the hardness of the sample rolled at 373 K at the same reduction in thickness,  $H_0$  is the hardness of the as-received sheet, and  $V_M$  is the volume fraction of martensite. Therefore, the difference between the hardness of the sample rolled at 300 K ( $H_{300}$ ) and  $\Delta H_{\gamma} + H_0$ , denoted by  $\Delta H_{\alpha'}$ , can be considered as a representation of the real effect of martensite on increasing hardness of the samples rolled at 300 K. The real effect of martensite, itself, can be divided to the effect of martensite phase as a hard phase and the work-hardening of martensite during cold rolling. Note that it is difficult to separate these effects from each other because the martensite phase forms by cold rolling and work-hardens simultaneously.

The outcome of the discussion based on Eq. (2) is shown in Figure 2, which reveals that the values of  $\Delta H_{\gamma}$  firstly increase by increasing rolling reduction, and then, since the amount of austenite declines, the values of  $\Delta H_{\gamma}$  decrease by further rolling. On the other hand, the effect of martensite ( $\Delta H_{\alpha'}$ ) continuously increases by rolling. The most significant aspect of this analysis is consideration of the variation of the amount of austenite and martensite on the hardening of the sheets.

The above findings are summarized in Figure 3 by consideration of the volume fraction of martensite. It can be seen that at low fractions of martensite, the effect of both work-hardening of austenite ( $\Delta H_{\gamma}$ ) and presence of martensite ( $\Delta H_{\alpha'}$ ) is comparable. However, by increasing the amount of martensite, the difference between  $\Delta H_{\gamma}$  and  $\Delta H_{\alpha'}$  becomes significant, which can be related to the increase in the amount of martensite as discussed above.

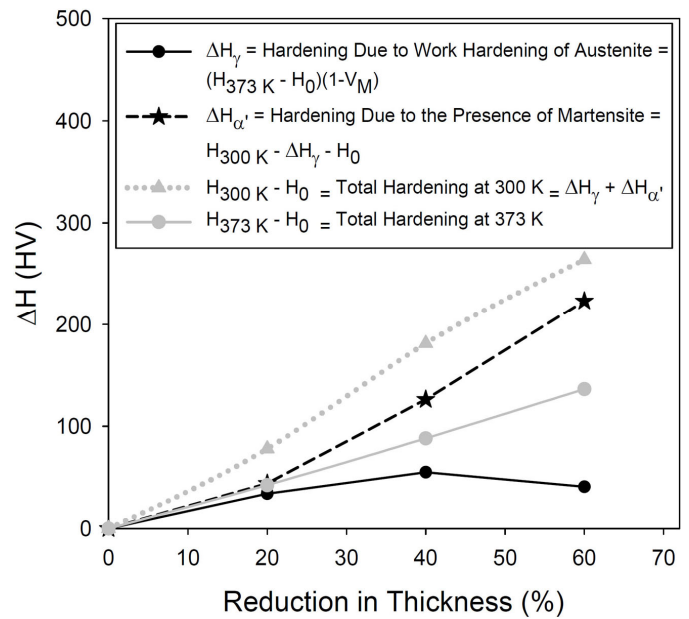


Fig. 2. The results of the calculations based on Eq. (2)

Accordingly, the difference between martensite effect ( $\Delta H_{\alpha'}$ ) and the total hardening ( $H_{300} - H_0$ ) decreases as can be clearly seen in Figure 3. Therefore, it can be surmised that the hardening effects of martensite and austenite has been separated, which might be important in understanding the behavior of austenitic stainless steels during cold rolling, where both austenite and martensite are present in the sheets after rolling.

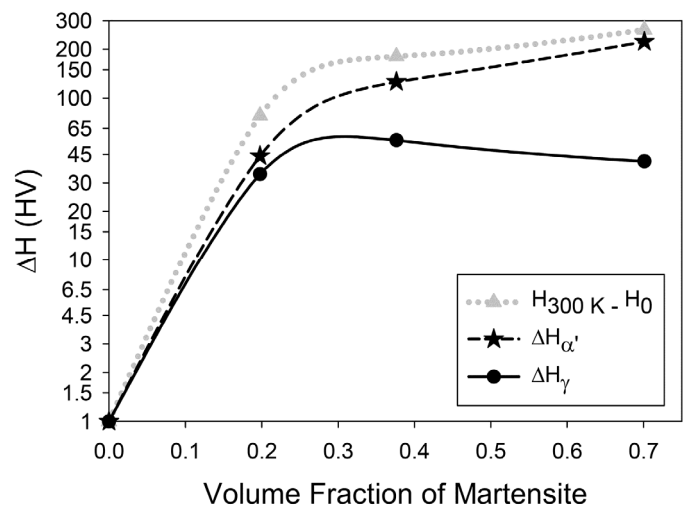


Fig. 3. The hardening effects versus martensite volume fraction

#### 5. Summary

In summary, the contributions of work-hardening of austenite and the presence of martensite on the hardening of an AISI 304L stainless steel were evaluated based on plastic deformation under different reductions in thickness at two rolling temperatures. The cold deformation temperatures of 300 K and 373 K were chosen to induce strain-hardening plus strain-induced

martensitic transformation in the former and strain-hardening in the latter. This made it possible to elucidate the real effects of strengthening mechanisms of metastable austenitic stainless steels during mechanical working.

## REFERENCES

- [1] K. Nagai, *Can. Metall. Q.* **44**, 187-194 (2005).
- [2] H. Mirzadeh, J.M. Cabrera, A. Najafizadeh, P.R. Calvillo, *Mater. Sci. Eng. A* **538**, 236-245 (2012).
- [3] N.D. Ryan, H.J. McQueen, J.J. Jonas, *Can. Metall. Q.* **22**, 369-378 (1983).
- [4] A. Järvenpää, M. Jaskari, J. Man, L.P. Karjalainen, *Mater. Charact.* **127**, 12-26 (2017).
- [5] H.R. Bakhsheshi-Rad, B. Haerian, A. Najafizadeh, M.H. Idris, M.R.A. Kadir, E. Hamzah, M. Daroonparvar, *Can. Metall. Q.* **52**, 449-457 (2013).
- [6] M. Naghizadeh, H. Mirzadeh, *Metall. Mater. Trans. A* **47**, 4210-4216 (2016).
- [7] D.M. Xu, G.Q. Lia, X.L. Wan, R.L. Xiong, G. Xu, K.M. Wu, M.C. Somani, R.D.K. Misra, *Mater. Sci. Eng. A* **688**, 407-415 (2017).
- [8] A. Kisko, A.S. Hamada, J. Talonen, D. Porter, L.P. Karjalainen, *Mater. Sci. Eng. A* **657**, 359-370 (2016).
- [9] C.Y. Lee, C.S. Yoo, A. Kermanpur, Y.K. Lee, *J. Alloy Compd.* **583**, 357-360 (2014).
- [10] P. Dastur, A. Zarei-Hanzaki, M.H. Pishbin, M. Moallemi, H.R. Abedi, *Mater. Sci. Eng. A* **696**, 511-519 (2017).
- [11] H. Kotan, K.A. Darling, *Mater. Sci. Eng. A* **686**, 168-175 (2017).
- [12] C. Lei, X. Deng, X. Li, Z. Wang, G. Wang, R.D.K. Misra, *J. Alloy Compd.* **689**, 718-725 (2016).
- [13] M. El-Tahawy, Y. Huang, H. Choi, H. Choe, J.L. Lábár, T.G. Langdon, J. Gubicza, *Mater. Sci. Eng. A* **682**, 323-331 (2017).
- [14] F. Borgioli, E. Galvanetto, T. Bacci, *Vacuum* **127**, 51-60 (2016).
- [15] K. Spencer, J.D. Embury, K.T. Conlon, M. Veron, Y. Brechet, *Mater. Sci. Eng. A* **387-389**, 873-81 (2004).
- [16] M. Shirdel, H. Mirzadeh, M.H. Parsa, *Mater. Charact.* **103**, 150-161 (2015).
- [17] H. Mirzadeh and A. Najafizadeh, *J. Alloy Compd.* **476**, 352-355 (2009).
- [18] J.R. McDermid, H.S. Zurob, Y. Bian, *Metall. Mater. Trans. A* **42**, 3627-3637 (2011).
- [19] X.L. Wu, M.X. Yang, F.P. Yuan, L. Chen, Y.T. Zhu, *Acta Mater.* **112**, 337-346 (2016).
- [20] H. Mirzadeh, *Metall. Mater. Trans. A* **46**, 4027-4037 (2015).
- [21] B. Fultz and J. Howe, *Transmission Electron Microscopy and Diffractometry of Materials*, 3rd ed., 2008 Springer, Berlin.